

Spherical collapse in $f(R)$ gravity

Jun-Qi Guo,^{1,*} Daoyan Wang,^{2,†} and Andrei V. Frolov^{1,‡}

¹ *Department of Physics, Simon Fraser University
8888 University Drive, Burnaby, BC V5A 1S6, Canada*

² *Department of Physics & Astronomy, University of British Columbia
6224 Agricultural Road, Vancouver, BC V6T 1Z1, Canada*

(Dated: June 2, 2022)

The spherical scalar collapse in $f(R)$ gravity is studied numerically in Einstein frame. The dark-energy-oriented $f(R)$ theory is a modification of general relativity at low-curvature scale. The scalar curvature decreases when the scalar field collapses to form a black hole. Correspondingly, gravity transits from general relativity to $f(R)$ gravity, and the scalar degree of freedom f' is released from a coupled state to a light state. Compared to the gravitational force from the scalar sphere (which collapses to form a black hole in a later stage), the left barrier of the potential for f' is not steep enough. As a result, near the singularity of the black hole, f' will cross the minimum of the potential and then approach zero. As the singularity is approached, the equations of motion are dominated by time derivative terms; the contributions from other terms, including those from the scalar fields, are negligible. The spacetime and the scalar fields are described by Kasner solution. These results support the Belinskii, Khalatnikov, and Lifschitz (BKL) conjecture well. The final state of the collapse is discussed.

PACS numbers: 04.25.dc, 04.25.dg, 04.50.Kd, 04.70.Bw

I. INTRODUCTION

General relativity is a milestone in gravitation. However, some problems in general relativity, e.g., the non-renormalizability of general relativity and the singularity problems in black hole physics and in the early Universe, imply that general relativity may not be the final gravitational theory. The theoretical and observational explorations in cosmology and astrophysics, e.g., inflation, the orbital velocities of galaxies in clusters and the cosmic acceleration, also encourage people to consider new gravitational theories [1, 2, 3, 4, 5]. Among various modified gravity theories, $f(R)$ gravity is a natural extension of general relativity. In this theory, the Ricci scalar in the Einstein-Hilbert action is replaced by an arbitrary function of the Ricci scalar,

$$S = \frac{1}{16\pi G} \int d^4x \sqrt{-g} f(R) + S_m, \quad (1)$$

where G is the Newtonian constant, and S_m is the matter term in the action [3, 4, 5]. The models of this type became popular in cosmology, with people trying to attribute the late-time accelerated expansion of the Universe to gravitational degrees of freedom. [See Refs. [6, 7] for reviews of $f(R)$ theory.]

Black hole physics and spherical collapse are important platforms from which to understand gravity. [For reviews of gravitational collapse and spacetime singularities, see Refs. [8, 9, 10, 11].] Historically, some static

solutions for black holes have been obtained analytically. The “no-hair” theorem states that a stationary black hole can be described by only a few parameters [12]. Hawking showed that stationary black holes as the final states of Brans-Dicke collapses are identical to those in general relativity [13]. In Ref. [14], a novel “no-hair” theorem was proven. In this theorem, the scalar field, surrounding an asymptotically flat, static, spherically symmetric black hole, is assumed to be minimally coupled to gravity, and to have a non-negative energy density. In this case, the black hole must be a Schwarzschild black hole. This result is also valid if the scalar field has a potential whose global minimum is zero. The possible black hole solutions were explored in scalar-tensor gravity, including $f(R)$ gravity, by Sotiriou and Faraoni. If black holes were to be isolated from the cosmological background, they would have a Schwarzschild solution [15].

As astrophysics black holes are expected to come from collapses of matter, studying collapse processes, especially spherical collapses due to simpleness, is an instructive way to explore black hole physics and to verify the results on stationary black holes as well. The Oppenheimer-Snyder solution provides an analytic description of the spherical dust collapse into a Schwarzschild black hole [16]. However, due to the complexity of non-linearity of Einstein field equations, in most other cases, the collapse solutions have to be searched for numerically. The simulations of spherical collapse in Brans-Dicke theory were implemented in Refs. [17, 18, 19], confirming Hawking’s conclusion that stationary black holes as the final states of Brans-Dicke collapses are identical to those in general relativity [13]. In Ref. [20], numerical integration of the Einstein equations outwards from the horizon was performed. The results strongly supported the new “no-hair” theorem

*Electronic address: jga35@sfu.ca

†Electronic address: dwang@phas.ubc.ca

‡Electronic address: frolov@sfu.ca

presented in Ref. [14]. Recently, the dynamics of single and binary black holes in scalar-tensor theories in the presence of a scalar field was studied in Ref. [21], in which the potential for scalar-tensor theories is set to zero and the source scalar field is assumed to have a constant gradient. Although $f(R)$ theory is equivalent to scalar-tensor theories, it is a unique type. In $f(R)$ theory, the potential is related to the function $f(R)$ or the Ricci scalar R by $V'(\chi) \equiv (2f - \chi R)/3$, with $\chi \equiv f'$. In dark-energy-oriented $f(R)$ gravity, the de Sitter curvature obtained from $V'(\chi) \equiv (2f - \chi R)/3 = 0$ is expected to drive the cosmic acceleration. Thus, the minimum of the potential cannot be zero. Therefore, the spherical collapse in $f(R)$ theory has rich phenomenology, and is worth exploring in depth, although some studies have been implemented in scalar-tensor theories. In Ref. [22], the gravitational collapse of a uniform dust cloud in $f(R)$ gravity was analysed; the scale factor and the collapsing time were computed. However, a general collapse in scalar-tensor theories (especially in $f(R)$ theory), in which the global minimum of the potential is non-zero, remains unexplored as of yet. In addition to black hole formation, large-scale structure is another possible end state of spherical collapse. In Refs. [23, 24], with the scalar fields being assumed to be quasistatic, simulations of dark matter halo formation were implemented in $f(R)$ gravity and Galileon gravity, respectively.

Another motivation comes from the study of the dynamics as one approaches the singularity. The Belinskii, Khalatnikov, and Lifschitz (BKL) conjecture states that as the singularity is approached, the dynamical terms will dominate the spatial terms in the Einstein field equations, the metric terms will dominate matter field terms, and the metric components and the matter fields are described by Kasner solution [25, 26, 27]. The BKL conjecture was verified numerically for the singularity formation in a closed cosmology in Refs. [28, 29]. It was also confirmed in Ref. [30] with a test scalar field approaching the singularity of a black hole, whose metric is described by a spatially flat dust Friedmann–Lemaître–Robertson–Walker spacetime. In Ref. [31], the BKL conjecture in the Hamiltonian framework was examined, in an attempt to understand the implications of the BKL conjecture to loop quantum gravity. In this paper, we consider a scalar field collapse in $f(R)$ gravity. We study the evolution of the spacetime, the physical scalar field ψ , and the scalar degree of freedom f' throughout the whole collapse process and also in the regime near the singularity.

We take the Hu-Sawicki model as a sample $f(R)$ model [4]. We perform the simulations in the double-null coordinate proposed by Christodoulou [32], because this coordinate has the horizon-penetration advantage and also allows us to study the global structure of spacetime. The results show that a black hole can be formed. During the collapse, the Ricci scalar decreases, the modification term in the function $f(R)$ becomes important, and the scalar field f' becomes light. The lightness of

f' and the gravity from the scalar sphere, which forms a black hole later, make the scalar field f' cross the minimum of the potential (also called a de Sitter point), and then approach zero near the singularity. In the equations of motion for the metric components and the scalar fields, the spatial terms are negligible. Thus, the equations of motion are decoupled, becoming ordinary differential equations with respect to the coordinate time. Compared to gravity, matter fields can also be neglected. These results support the BKL conjecture.

In the static black hole solution in $f(R)$ gravity, the scalar field f' sits at the minimum of the potential. However, f' can be easily perturbed because the Ricci scalar R is low and then f' is very light. As a result, it is challenging to obtain a static de Sitter-Schwarzschild solution in the simulations of spherical collapse. Instead, one can study the possible final state of the collapse in an approximate but simpler way. When a black hole forms, the contribution from dark energy is much smaller than that from the Schwarzschild black hole. Therefore, one may simply check the dynamics of the scalar fields in a fixed Schwarzschild background. The preliminary results show that, in Jordan frame, f' can cross the minimum of the potential and approach $-\infty$. Consequently, even in this approach, it remains nontrivial to obtain the final states of the scalar fields.

To a large extent, the features of $f(R)$ theory are defined by the shape of the potential. The local tests and the cosmological dynamics of $f(R)$ theory are closely related to the right side and the minimum area of the potential [33, 34, 35, 36]. In the early Universe, the scalar degree of freedom f' is coupled to the matter density. In the later evolution, f' is decoupled from the matter density and goes down toward the minimum of the potential, and eventually stops at the minimum after some oscillations. Interestingly, the study of the collapse process draws one's attention to the left side of the potential.

The paper is organized as follows. In Sec. II, we introduce the framework of the collapse, including the formalism of $f(R)$ theory, the double-null coordinate, and the Hu-Sawicki model. In Sec. III, we set up the numerical structure, including discretizations of the equations of motion, defining initial and boundary conditions, and implementing the numerical tests. In Sec. IV, the numerical results are presented. In Sec. V, we study the dynamics of two test scalar fields in a Schwarzschild metric. Section VI summarizes our work.

II. FRAMEWORK

In this section, we build the framework of the spherical scalar collapse in $f(R)$ theory. For numerical stability reasons, $f(R)$ gravity is transformed from Jordan frame into Einstein frame. In order to study the global structure of the spacetime, and the dynamics of the spacetime and the source fields near the singularity, we simulate the collapse in the double-null coordinate. A typical $f(R)$

model, the Hu-Sawicki model, is chosen as an example. This paper gives the first reported results on numerical simulations of fully dynamical spherical collapse in $f(R)$ gravity towards black hole formation.

A. $f(R)$ theory

The equivalent of the Einstein equation in $f(R)$ gravity reads

$$f'R_{\mu\nu} - \frac{1}{2}fg_{\mu\nu} - (\nabla_\mu \nabla_\nu - g_{\mu\nu}\square)f' = 8\pi GT_{\mu\nu}, \quad (2)$$

where f' denotes the derivative of the function f with respect to its argument R , and \square is the usual notation for the covariant D'Alembert operator $\square \equiv \nabla_\alpha \nabla^\alpha$. Compared to general relativity, $f(R)$ gravity has one extra scalar degree of freedom, f' . The dynamics of this degree of freedom is determined by the trace of Eq. (2)

$$\square f' = \frac{1}{3}(2f - f'R) + \frac{8\pi G}{3}T, \quad (3)$$

where T is the trace of the stress-energy tensor $T_{\mu\nu}$. Identifying f' with a scalar degree of freedom by

$$\chi \equiv \frac{df}{dR}, \quad (4)$$

and defining a potential $U(\chi)$ by

$$U'(\chi) \equiv \frac{dU}{d\chi} = \frac{1}{3}(2f - \chi R), \quad (5)$$

one can rewrite Eq. (3) as

$$\square \chi = U'(\chi) + \frac{8\pi G}{3}T. \quad (6)$$

In order to operate $f(R)$ gravity, it is instructive to cast the formulation of $f(R)$ gravity into a format similar to that of general relativity. We rewrite Eq. (2) as

$$G_{\mu\nu} = 8\pi G \left(T_{\mu\nu} + T_{\mu\nu}^{(\text{eff})} \right), \quad (7)$$

where

$$8\pi GT_{\mu\nu}^{(\text{eff})} = \frac{f - f'R}{2}g_{\mu\nu} + (\nabla_\mu \nabla_\nu - g_{\mu\nu}\square)f' + (1 - f')G_{\mu\nu}. \quad (8)$$

$T_{(\text{eff})}^{\mu\nu}$ is the energy-momentum tensor of the effective dark energy. It is guaranteed to be conserved, $T_{(\text{eff});\nu}^{\mu\nu} = 0$. Note that there are second-order derivatives of f' in $T_{\mu\nu}^{(\text{eff})}$. These terms can easily make the numerical code unstable. Instead, we transform $f(R)$ gravity from the current frame, which is usually called Jordan frame, into Einstein frame, in which second-order derivatives of f' are absent.

Rescaling χ by

$$\kappa\phi \equiv \sqrt{3/2} \ln \chi, \quad (9)$$

one obtains the corresponding action of $f(R)$ gravity in Einstein frame [7]

$$S_E = \int d^4x \sqrt{-\tilde{g}} \left[\frac{1}{2\kappa^2} \tilde{R} - \frac{1}{2} \tilde{g}^{\mu\nu} \partial_\mu \phi \partial_\nu \phi - V(\phi) \right] + \int d^4x \mathcal{L}_M(\tilde{g}_{\mu\nu}/\chi(\phi), \psi), \quad (10)$$

where $\kappa = \sqrt{8\pi G}$, $\tilde{g}_{\mu\nu} = \chi \cdot g_{\mu\nu}$, $V(\phi) \equiv (\chi R - f)/(2\kappa^2\chi^2)$, and a tilde denotes that the quantities are in Einstein frame. The Einstein fields equations are

$$\tilde{G}_{\mu\nu} = \kappa^2 \left[\tilde{T}_{\mu\nu}^{(\phi)} + \tilde{T}_{\mu\nu}^{(M)} \right], \quad (11)$$

where

$$\tilde{T}_{\mu\nu}^{(\phi)} = \partial_\mu \phi \partial_\nu \phi - \tilde{g}_{\mu\nu} \left[\frac{1}{2} \tilde{g}^{\alpha\beta} \partial_\alpha \phi \partial_\beta \phi + V(\phi) \right], \quad (12)$$

$$\tilde{T}_{\mu\nu}^{(M)} = \frac{T_{\mu\nu}^{(M)}}{\chi}. \quad (13)$$

$T_{\mu\nu}^{(M)}$ is the ordinary energy-momentum tensor of the physical matter field in terms of $g_{\mu\nu}$ in Jordan frame. We take a massless scalar field ψ as the matter field for the collapse. Its energy-momentum tensor in Einstein frame is

$$\tilde{T}_{\mu\nu}^{(M)} = \frac{1}{\chi} \left(\partial_\mu \psi \partial_\nu \psi - \frac{1}{2} g_{\mu\nu} g^{\alpha\beta} \partial_\alpha \psi \partial_\beta \psi \right), \quad (14)$$

which gives $\tilde{T}^{(M)} = -\chi^{-1} \cdot \tilde{g}^{\alpha\beta} \partial_\alpha \psi \partial_\beta \psi$. The equations of motion for ϕ and ψ can be derived from the Lagrange equations as

$$\tilde{\square} \phi - V'(\phi) + \kappa Q \tilde{T}^{(M)} = 0, \quad (15)$$

$$\tilde{\square} \psi - \sqrt{2/3} \kappa \tilde{g}^{\mu\nu} \partial_\mu \phi \partial_\nu \psi = 0, \quad (16)$$

where $Q \equiv -(\chi_{,\phi})/(2\kappa\chi) = -1/\sqrt{6}$, and $\tilde{T}^{(M)} \equiv \tilde{g}^{\mu\nu} \tilde{T}_{\mu\nu}^{(M)}$. In Einstein frame, the potential for ϕ is written as

$$V(\phi) = \frac{\chi R - f}{2\kappa^2 \chi^2}. \quad (17)$$

Then we have

$$V'(\phi) = \frac{dV}{d\chi} \cdot \frac{d\chi}{d\phi} = \frac{1}{\sqrt{6}} \frac{2f - \chi R}{\kappa \chi^2}. \quad (18)$$

B. Coordinate system

We are interested in the singularity formation, the dynamics of the spacetime and the source fields near the singularity, and the global structure of the spacetime.

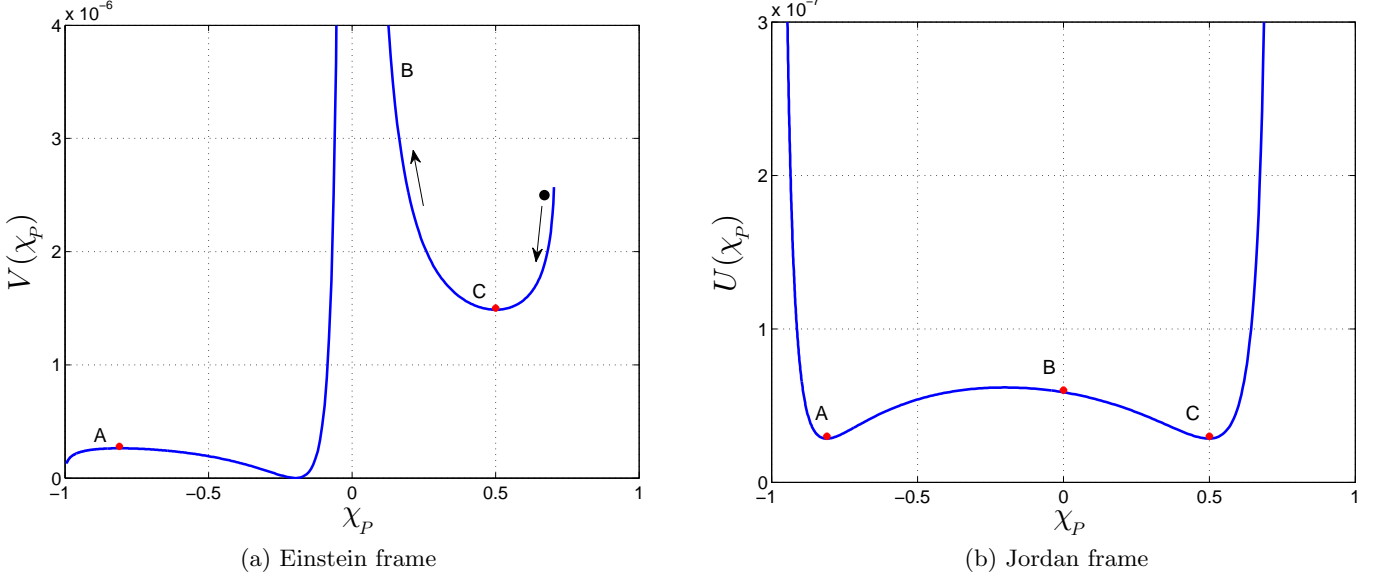


FIG. 1: The potentials in Einstein frame and Jordan frame for the Hu-Sawicki model. χ_P is a compactified coordinate obtained via the Poincaré transformation, $\chi_P = \chi/\sqrt{1+\chi^2}$, with $\chi \equiv f'$. The potential $V(\chi(\phi))$ in Einstein frame is defined by Eq. (25), and the potential $U(\chi)$ in Jordan frame is defined by Eq. (5).

The double-null coordinate described by Eq. (19) is an ideal choice to realize these objectives [32].

$$\begin{aligned} ds^2 &= e^{-2\sigma}(-dt^2 + dx^2) + r^2 d\Omega^2, \\ &= -4e^{-2\sigma} du dv + r^2 d\Omega^2, \end{aligned} \quad (19)$$

where $u(= (t-x)/2 = \text{Const.})$ and $v(= (t+x)/2 = \text{Const.})$ are outgoing and ingoing characteristics, respectively. The two-manifold metric

$$d\gamma^2 = e^{-2\sigma}(-dt^2 + dx^2) = -4e^{-2\sigma} du dv \quad (20)$$

is conformally flat. The double-null coordinate can cover the entire spacetime and penetrate the horizon, thus allowing us to study the global structure of the spacetime and the dynamics of the metric components and the source fields near the singularity as well. Moreover, in this coordinate, one can know the speed of information propagation everywhere in advance.

The metric (19) is invariant for the rescaling $u \rightarrow U(u), v \rightarrow V(v)$. We fix this gauge freedom by setting up initial and boundary conditions at known coordinate locations.

C. Hu-Sawicki model

In the study of the scalar collapse in $f(R)$ gravity, we take the Hu-Sawicki $f(R)$ model as an example. This model reads [4]

$$f(R) = R - \Lambda \frac{C_1 R^n}{C_2 R^n + \Lambda^n}, \quad (21)$$

where C_1 and C_2 are dimensionless parameters, $\Lambda = 8\pi G \bar{\rho}_0/3$, and $\bar{\rho}_0$ is the average matter density of the

current Universe. We consider one of the simplest versions of this model, i.e., $n = 1$,

$$f(R) = R - \frac{C\Lambda R}{R + \Lambda}, \quad (22)$$

where C is a dimensionless parameter. In this model,

$$f' = 1 - \frac{C\Lambda^2}{(R + \Lambda)^2}, \quad (23)$$

$$R = \Lambda \left[\sqrt{\frac{C}{1-f'}} - 1 \right], \quad (24)$$

$$V(\phi) = \frac{C\Lambda R^2}{2\kappa^2 f'^2 (R + \Lambda)^2}, \quad (25)$$

$$V'(\phi) = \frac{R^3}{\sqrt{6}\kappa f'^2 (R + \Lambda)^2} \left[1 + (1-C) \frac{\Lambda}{R} \left(2 + \frac{\Lambda}{R} \right) \right]. \quad (26)$$

Equations (23) and (26) show that as long as the matter density is much greater than Λ , the curvature R will trace the matter density well, f' will be close to 1 but not cross 1, and general relativity will be restored. As implied in Eq. (26), in order to make sure that the de Sitter curvature, for which $V'(\phi) = 0$, has a positive value, the parameter C needs to be greater than 1. In this paper, we set C and Λ to 1.2 and 5×10^{-6} , respectively. The potential in Einstein frame defined by Eq. (25) and the potential in Jordan frame defined by Eq. (5) are plotted in Figs. 1(a) and 1(b), respectively. As shown in Eq. (25)

and Fig. 1(a), the potential in Einstein frame has two poles, ($f' = 0, R = (\sqrt{c} - 1)\Lambda$) and ($f' = -\infty, R = -\Lambda$). However, the potential in Jordan frame has only one pole ($f' = -\infty, R = -\Lambda$), see Eq. (5) and Fig. 1(b).

III. NUMERICAL SET-UP

In this section, we present the numerical formalisms, including field equations, initial conditions, boundary conditions, discretization scheme, and numerical tests. The numerical code used in the paper is a generalized version of the one implemented by one of the authors [37].

A. Field equations

In this paper, we set $8\pi G$ to 1. Then, in the double-null coordinate (19), using $G_t^t + G_x^x = T^{(\phi)}_t{}^t + T^{(\phi)}_x{}^x + T^{(\psi)}_t{}^t + T^{(\psi)}_x{}^x$, one obtains the equation of motion for the metric component r ,

$$r(-r_{,tt} + r_{,xx}) + (-r_{,t}^2 + r_{,x}^2) = e^{-2\sigma}(1 - r^2 V). \quad (27)$$

Equation (27) involves a delicate cancelation of terms at both small and large r , which makes it susceptible to discretization errors. In order to avoid this problem, when r is not too large, we define $\eta \equiv r^2$, and integrate the equation of motion for η , instead. The equation of motion for η can be obtained by rewriting Eq. (27) as

$$-\eta_{,tt} + \eta_{,xx} = 2e^{-2\sigma} \left(1 - \frac{1}{2}r^2 V\right). \quad (28)$$

When r is very large, the delicate cancellation problem can be avoided by using a new variable $\rho \equiv 1/r$, instead. $G_\theta^\theta = T_\theta^\theta$ provides the equation of motion for σ ,

$$\begin{aligned} & -\sigma_{,tt} + \sigma_{,xx} - \frac{-r_{,tt} + r_{,xx}}{r} - \frac{1}{2}(-\phi_{,t}^2 + \phi_{,x}^2) \\ & - \frac{1}{2\chi}(-\psi_{,t}^2 + \psi_{,x}^2) = e^{-2\sigma} V. \end{aligned} \quad (29)$$

In the double-null coordinate, the dynamical equations for ϕ (15) and ψ (16) become, respectively,

$$\begin{aligned} & (-\phi_{,tt} + \phi_{,xx}) + \frac{2}{r}(-r_{,t}\phi_{,t} + r_{,x}\phi_{,x}) \\ & = e^{-2\sigma} \left[V'(\phi) + \frac{1}{\sqrt{6}}\kappa T^{(\psi)} \right], \end{aligned} \quad (30)$$

$$\begin{aligned} & (-\psi_{,tt} + \psi_{,xx}) + \frac{2}{r}(-r_{,t}\psi_{,t} + r_{,x}\psi_{,x}) \\ & = \sqrt{\frac{2}{3}} \kappa(-\phi_{,t}\psi_{,t} + \phi_{,x}\psi_{,x}), \end{aligned} \quad (31)$$

where

$$T^{(\psi)} = -\frac{1}{\chi}e^{2\sigma}(-\psi_{,t}^2 + \psi_{,x}^2). \quad (32)$$

The $\{uu\}$ and $\{vv\}$ components of the Einstein equations yield the constraint equations,

$$r_{,uu} + 2\sigma_{,u}r_{,u} = -\frac{r}{2}(\phi_{,u}^2 + \psi_{,u}^2/\chi), \quad (33)$$

$$r_{,vv} + 2\sigma_{,v}r_{,v} = -\frac{r}{2}(\phi_{,v}^2 + \psi_{,v}^2/\chi). \quad (34)$$

Via the definitions of $u = (t - x)/2$ and $v = (t + x)/2$, the constraint equations can be expressed in (t, x) coordinates. Equations (34) – (33) and (34) + (33) generate the constraint equations for $\{xt\}$ and $\{xx\} + \{tt\}$ components, respectively,

$$r_{,xt} + r_{,t}\sigma_{,x} + r_{,x}\sigma_{,t} + \frac{r}{2}\phi_{,t}\phi_{,x} + \frac{r}{2f'}\psi_{,t}\psi_{,x} = 0, \quad (35)$$

$$r_{,tt} + r_{,xx} + 2r_{,t}\sigma_{,t} + 2r_{,x}\sigma_{,x} + \frac{r}{2}(\phi_{,x}^2 + \phi_{,t}^2) + \frac{r}{2f'}(\psi_{,x}^2 + \psi_{,t}^2) = 0. \quad (36)$$

Regarding the equation of motion for σ , the term $(-r_{,tt} + r_{,xx})/r$ in (29) can create big errors near the center $r \approx 0$. To circumvent this problem, we use the constraint equation (33) alternatively. A new variable g is defined as

$$g = -2\sigma - \ln(-r_{,u}). \quad (37)$$

Then, Eq. (33) can be written as the equation of motion for g ,

$$g_{,u} = \frac{r}{2} \frac{\phi_{,u}^2 + \psi_{,u}^2/\chi}{r_{,u}}. \quad (38)$$

In the numerical integration, once the value of g at the advanced level is obtained, the value of σ at the current level will be computed from Eq. (37).

B. Initial conditions

For any dynamical system whose evolution is governed by second-order time derivative equation, its evolution is uniquely determined by setting the value of the dynamical variable, and its first-order time derivative, at any given instant. Here we set the first-order time derivatives $r_{,t}$ and $\sigma_{,t}$ to zero at $t = 0$, and allow the fields ϕ and ψ to have small initial speeds, with the constraint equation (35) being satisfied.

We set the initial value of $\psi(r)$ at $t = 0$ as

$$\psi(r) = A \cdot \tanh \left[\frac{(r - r_0)^2}{B^2} \right]. \quad (39)$$

The initial value of $\phi(r)$ can be arbitrary as long as it is negative. [See Eq. (9) and note that $\chi \equiv f' < 1$.] Here we choose its value as that in static system and weak-field limit $r = x$ and $\sigma = 0$. In this case, the equation of motion for ϕ , Eq. (30), becomes

$$\frac{d^2\phi}{dr^2} + \frac{2}{r} \frac{d\phi}{dr} = \left[V'(\phi) + \frac{1}{\sqrt{6}} \kappa T^{(\psi)} \right]. \quad (40)$$

We solve this equation for initial $\phi(r)$ with Newton's iteration method.

We define a local mass by

$$p \equiv g^{\mu\nu} r_{,\mu} r_{,\nu} = 1 - \frac{2m}{r}. \quad (41)$$

Using $r_{,t} = 0$, $x = v - u$, and $t = u + v$, we have $r_{,u} = -r_{,x}$ at $t = 0$. Then, in the double-null coordinate described by (19), Eq. (41) implies that

$$e^{-2\sigma} = \frac{r_{,x}^2}{p}. \quad (42)$$

On the other hand, from Eq. (37), one obtains at $t = 0$,

$$r_{,u} = -r_{,x} = -e^{-2\sigma} e^{-g}. \quad (43)$$

Combination of Eqs. (42) and (43) provides the equation for r ,

$$r_{,x} = \left(1 - \frac{2m}{r} \right) e^g. \quad (44)$$

Assigning that $r_{,t} = \sigma_{,t} = 0$ and $r_{,tt} + r\phi_{,t}^2/2 + r\psi_{,t}^2/(2f') = 0$ at $t = 0$, Eqs. (36) and (27) become, respectively,

$$r_{,xx} + 2r_{,x}\sigma_{,x} + \frac{r}{2} \left(\phi_{,x}^2 + \frac{\psi_{,x}^2}{\chi} \right) = 0, \quad (45)$$

$$e^{2\sigma} r_{,xx} = -rV + \frac{2m}{r^2} + e^{2\sigma} r_{,tt}. \quad (46)$$

Differentiating Eq. (42) with respect to r yields

$$e^{2\sigma} (2\sigma_{,x} r_{,x} + 2r_{,xx}) = -\frac{2m_{,r}}{r} + \frac{2m}{r^2}. \quad (47)$$

Substituting Eqs. (45) and (46) into Eq. (47) generates the equation for m

$$m_{,r} = \frac{r^2}{2} \left[V + \frac{1}{2} e^{2\sigma} \left(\phi_{,x}^2 + \frac{\psi_{,x}^2}{\chi} \right) - e^{2\sigma} \frac{r_{,tt}}{r} \right]. \quad (48)$$

Moreover, with Eq. (42), we have

$$\begin{aligned} e^{2\sigma} r^2 \left(\phi_{,x}^2 + \frac{\psi_{,x}^2}{\chi} \right) &= e^{2\sigma} r^2 \left(\phi_{,r}^2 + \frac{\psi_{,r}^2}{\chi} \right) r_{,x}^2 \\ &= r^2 \left(\phi_{,r}^2 + \frac{\psi_{,r}^2}{\chi} \right) \left(1 - \frac{2m}{r} \right). \end{aligned}$$

Then Eq. (48) can be rewritten as

$$\begin{aligned} m_{,r} + \frac{1}{2} m r \left(\phi_{,r}^2 + \frac{\psi_{,r}^2}{\chi} \right) \\ = \frac{r^2}{2} \left[V + \frac{1}{2} \left(\phi_{,r}^2 + \frac{\psi_{,r}^2}{\chi} \right) - e^{2\sigma} \frac{r_{,tt}}{r} \right]. \end{aligned} \quad (49)$$

The equation for g at $t = 0$ can be obtained from Eq. (38),

$$g_{,r} = \frac{r}{2} \left(\phi_{,r}^2 + \frac{\psi_{,r}^2}{\chi} \right). \quad (50)$$

We obtain the initial values of r , m and g at $t = 0$ by integrating Eqs. (44), (49) and (50) via fourth order Runge-Kutta method.

C. Boundary conditions

Regarding the inter boundary conditions at $x = 0$, r is always set to zero. In order to make Eqs. (30) and (31) be regular at $r = x = 0$, we enforce ϕ and ψ to satisfy the following conditions:

$$-r_{,t}\phi_{,t} + r_{,x}\phi_{,x} = 0, \quad (51)$$

$$-r_{,t}\psi_{,t} + r_{,x}\psi_{,x} = 0. \quad (52)$$

The boundary condition for g at $r = 0$ can be obtained from Eq. (38).

Considering the outer boundary, since one cannot include infinity on the grid, one needs to put a cutoff at x , where the radius r is set to a constant. In this paper, we are interested in both the dynamics near the singularity of the black hole and the final state of the collapse. The simulations of the dynamics near the singularity will not be affected by the outer boundary conditions, as long as the spatial range of x is large enough compared to the time range needed for a black hole formation. For the moment, we simply set up the outer boundary conditions at $x = x_{\text{cutoff}}$ as follows. We let ϕ take the de Sitter value, and let $dg/dx = d\psi/dx = 0$.

D. Discretization scheme

The leapfrog integration scheme is implemented in this paper, which is second order accurate and non-dissipative. With the demonstration of Fig. 2 and using the variable ϕ as an example, our discretization scheme is expressed below.

$$\begin{aligned} \frac{d\phi}{dt} &= \frac{\phi_{\text{up}} - \phi_{\text{dn}}}{2\Delta t}, & \frac{d\phi}{dx} &= \frac{\phi_{\text{rt}} - \phi_{\text{lt}}}{2\Delta x}, \\ \frac{d^2\phi}{dt^2} &= \frac{\phi_{\text{up}} - 2\phi_{\text{hr}} + \phi_{\text{dn}}}{(\Delta t)^2}, & \frac{d^2\phi}{dx^2} &= \frac{\phi_{\text{lt}} - 2\phi_{\text{hr}} + \phi_{\text{rt}}}{(\Delta x)^2}, \\ \frac{d^2\phi}{dxdt} &= \frac{\phi_{\text{ur}} - \phi_{\text{ul}} - \phi_{\text{dr}} + \phi_{\text{dl}}}{(4\Delta x\Delta t)}. \end{aligned}$$

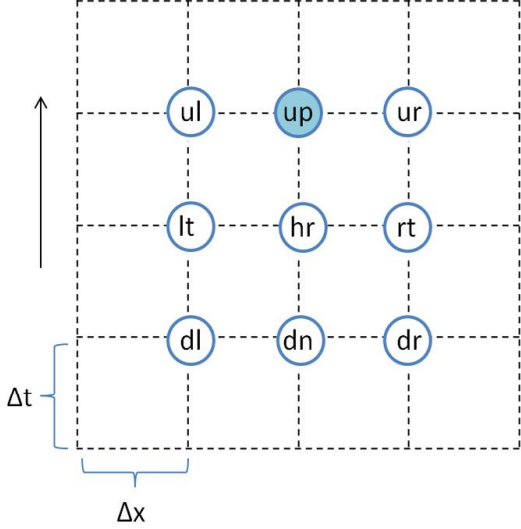


FIG. 2: Numerical evolution scheme.

In this paper, we let the temporal and the spatial grid distances be equal, $\Delta t = \Delta x$.

The equations of motion (28) for r , (30) for ϕ , and (31) for ψ are coupled. Newton's iteration method can be employed to solve this problem [38]. The initial conditions provide the data at the levels of “down” and “here”, and we need to obtain the data on the level of “up”. We take the values at the level of “here” to be the initial guess for the level of “up”. Then, we update the values at the level of “up” using the following iteration (taking ϕ as an example),

$$\phi_{\text{up}}^{\text{new}} = \phi_{\text{up}} - \frac{G(\phi_{\text{up}})}{J(\phi_{\text{up}})}, \quad (53)$$

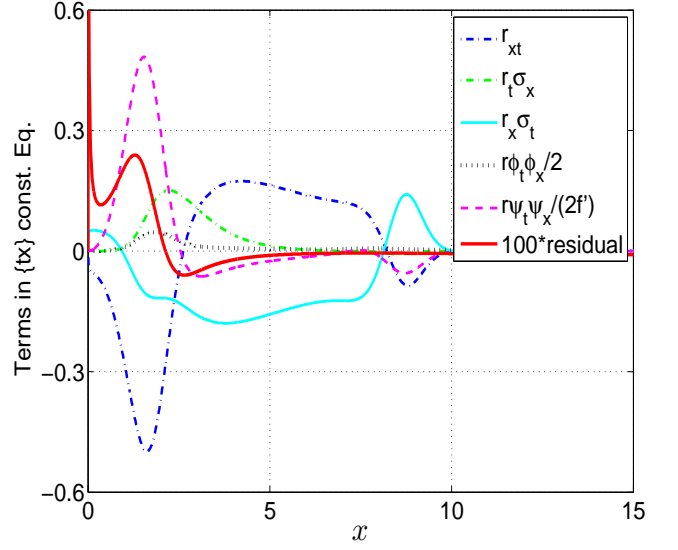
where $G(\phi_{\text{up}})$ is the residual of the differential equation for the function ϕ_{up} , and $J(\phi_{\text{up}})$ is the Jacobian defined by

$$J(\phi_{\text{up}}) = \frac{\partial G(\phi_{\text{up}})}{\partial \phi_{\text{up}}}. \quad (54)$$

We do the iterations for all of the coupled variables one by one, and run the iteration loops until the desired accuracies are achieved.

E. Numerical tests

The accuracies of the discretized equations of motion used in the simulations are checked. In the simulations, the grid distance Δx is set to 0.002. The relative errors are about 10^{-4} for r , 10^{-10} for ϕ and ψ , see Fig. 7. The equation of motion for g (38) is satisfied identically since it is solved directly. The accuracy for σ is about 10^{-3} , as shown in Fig. 7(b). As demonstrated in Fig. 3, the relative error for the $\{tx\}$ component constraint equation

FIG. 3: (Color online) The $\{xt\}$ constraint equation (35) when the coordinate time t is equal to 3.5. The relative error is around 0.003.

(35) is around 0.003. We will improve the accuracies later.

We do convergence tests via simulations with different grid sizes [39, 40]. If the numerical solution converges, the relation between the different numerical solutions and the real one can be expressed by

$$F_{\text{real}} = F^h + \mathcal{O}(h^n), \quad (55)$$

where n is the convergence order and F^h is the numerical solution with step size h . Then for step sizes equal to $h/2$ and $h/4$, we have

$$F_{\text{real}} = F^{h/2} + \mathcal{O}((h/2)^n), \quad (56)$$

$$F_{\text{real}} = F^{h/4} + \mathcal{O}((h/4)^n). \quad (57)$$

Defining $c_1 \equiv F^h - F^{h/2}$ and $c_2 \equiv F^{h/2} - F^{h/4}$, one can obtain the convergence rate

$$n = \log_2 \left(\frac{c_1}{c_2} \right). \quad (58)$$

The convergence tests for $\eta \equiv r^2$, g , ϕ , and ψ are investigated, and they are all close to 1 in the simulations. Noting that the leap-frog scheme is second-order accurate. The reason why the convergence order is equal to one rather than two is related to the initial conditions. We will improve this aspect later.

IV. RESULTS

A black hole formation from the scalar collapse in $f(R)$ gravity is obtained in this paper. Before the collapse,

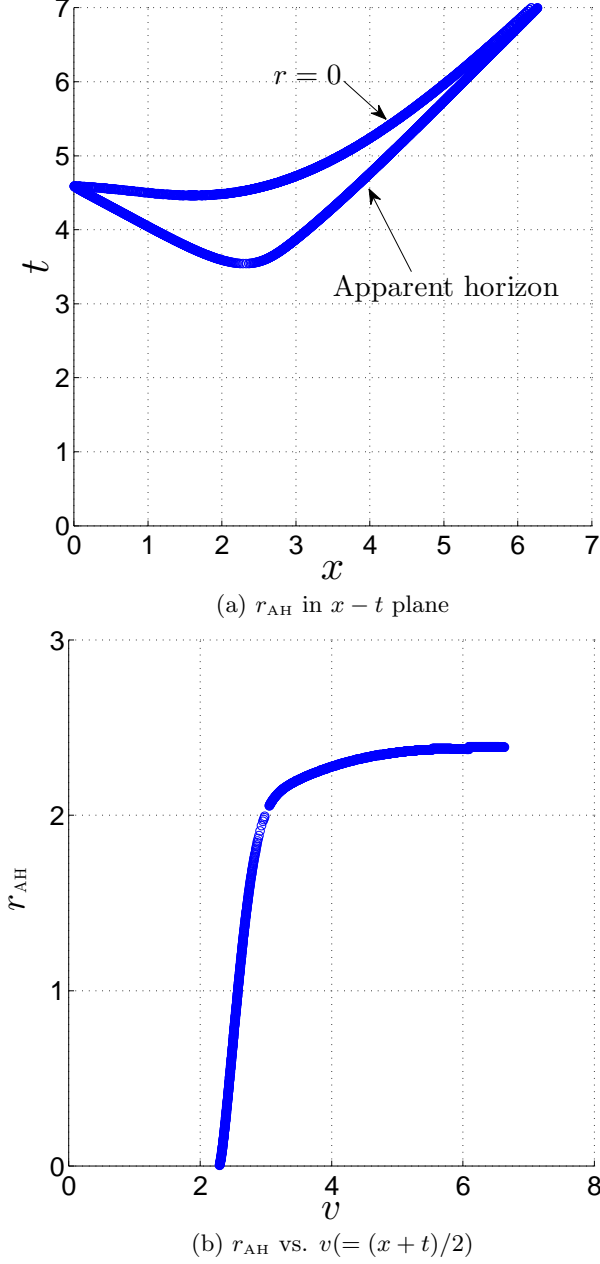


FIG. 4: Apparent horizon of the black hole obtained from the spherical collapse.

near the sphere, f' stays at the right side of the potential due to the balance between $U'(f')$ and the force from the physical scalar field ψ . During the collapse, the force from ψ decreases and changes direction in a later stage. Correspondingly, f' rolls down the potential and then crosses the minimum of the potential, as depicted in Fig. 1. If the energy carried by the scalar field ψ is small enough, the field f' will oscillate and eventually stop at the minimum of the potential. Simultaneously, the field ψ disperses. One obtains a de Sitter space. However, if the scalar field ψ carries enough energy, a black hole will

be formed. In our numerical simulation, a singularity surrounded by an apparent horizon is formed, as shown in Fig. 4. Therefore, a black hole is formed. The evolutions of r , f' , ψ are shown in Fig. 5. During the collapse, the Ricci scalar R in Jordan frame decreases, as shown in Fig. 5(d), and the field f' becomes light. Compared to gravity from the singularity, the left side of the potential $U(f')$ is not steep enough to stop f' from running in the left direction. Consequently, the field f' rolls down from its initial value which is close to 1, crosses the de Sitter point, and asymptotes to but does not cross zero near the singularity, as shown in Fig. 5(b).

The dynamics near the singularity is expressed by the universal Kasner solution [26]. The four dimensional homogeneous but anisotropic Kasner solution with a massless scalar field ζ can be described as follows [41]:

$$ds^2 = -d\tau^2 + \sum_{i=1}^3 \tau^{2p_i} dx_i^2,$$

$$p_1 + p_2 + p_3 = 0,$$

$$p_1^2 + p_2^2 + p_3^2 = 1 - q^2,$$

$$\zeta = q \ln \tau,$$

where the parameter q describes the contribution from the field ζ . The behavior of a test massive scalar field near the singularity in the spacetime of the Oppenheimer-Snyder collapse [16] was simulated in Ref. [30]. The results confirmed the BKL conjecture for an asymptotically flat spacetime. In the scalar collapse in $f(R)$ gravity that we studied in this paper, two scalar fields are present. One of them, ψ , is massless, and the other one, ϕ , is very light although it has a mass. Moreover, the spacetime has an asymptotic de Sitter solution. The results demonstrate that the metric components and both of the two fields are described by Kasner solution.

$$r \propto \tau^{\beta_1} + \text{Const},$$

$$e^{-2\sigma} \propto \tau^{\beta_2} + \text{Const},$$

$$\phi \propto q_1 \ln \tau + \text{Const},$$

$$\psi \propto q_2 \ln \tau + \text{Const},$$

where β_1 , β_2 , q_1 , and q_2 are constant parameters. The quantity τ is defined as follows. Set τ to zero as one hits the singularity and define $d\tau = -e^{-2\sigma} dt$. Then, one can write $e^{-2\sigma}$, ϕ and ψ as functions of r .

$$e^{-2\sigma} \propto r^{\beta_3} + \text{Const},$$

$$\phi \propto q_3 \ln r + \text{Const},$$

$$\psi \propto q_4 \ln r + \text{Const}.$$

These are shown in Fig. 6.

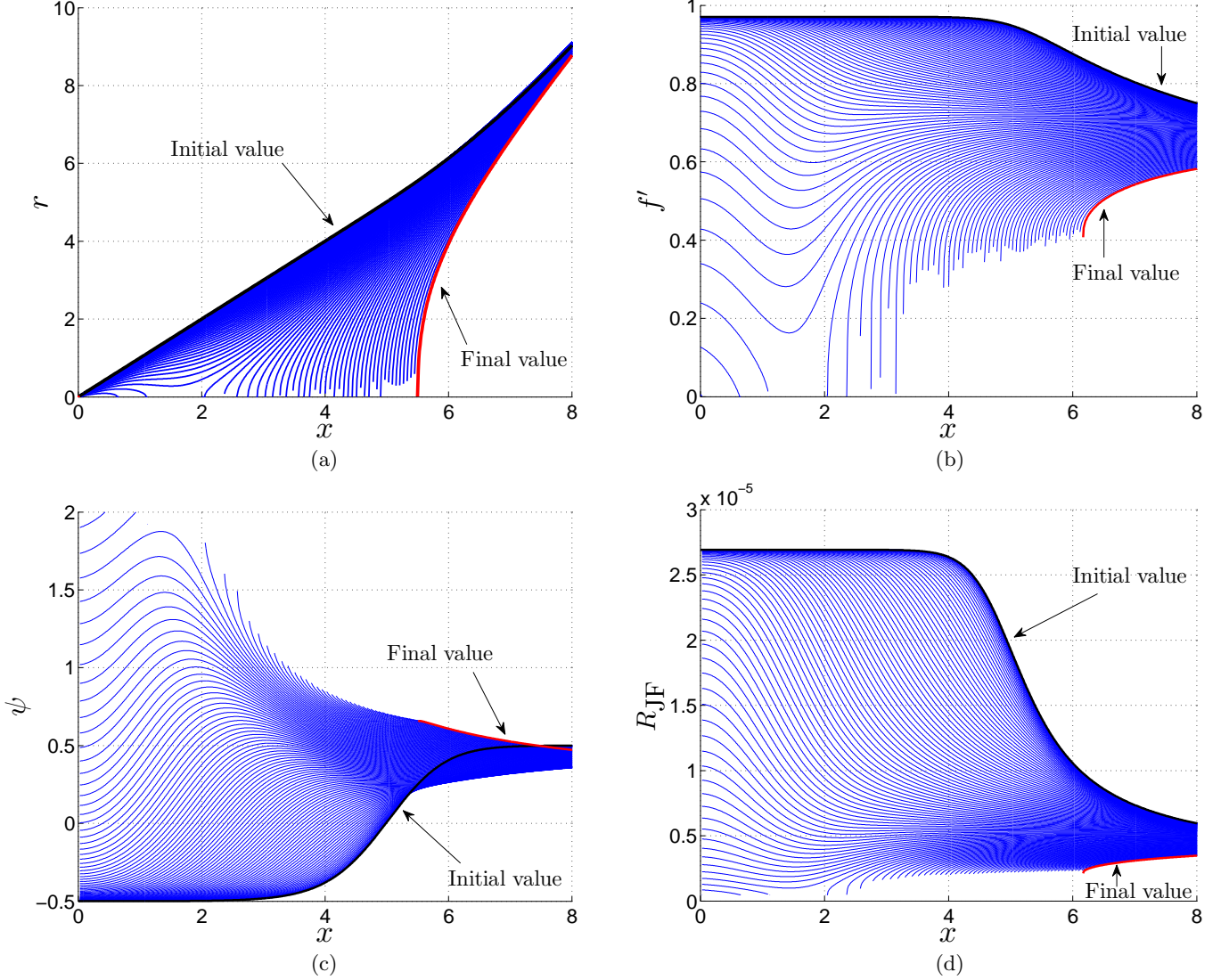


FIG. 5: The evolutions of the metric components and the scalar fields on consecutive time slices. (a) r . (b) f' . During the collapse, f' crosses the de Sitter value and approaches zero near the singularity. (c) ψ . (d) Ricci scalar in Jordan frame. Near the boundary of the scalar sphere, the Ricci scalar moves from a large value at the initial state to a very small value as one moves to the singularity. Correspondingly, the gravity transits from general relativity into $f(R)$ gravity, and the scalar degree of freedom f' becomes light.

As stated by the BKL conjecture [25], near the singularity of the black hole, in the equations of motion, the spatial derivatives can be neglected. Thus, the equations of motion transit from partial differential equations into ordinary differential equations with respect to the coordinate time. Moreover, if some matter fields are present in the collapse, their contributions can also be neglected. These statements are supported by our numerical results shown in Fig. 7. Near the singularity, the equations of motion for η , σ , ϕ , and ψ are reduced to

$$\eta_{,tt} + 2e^{-2\sigma} \approx 0, \quad (59)$$

$$\sigma_{,tt} - \frac{r_{,tt}}{r} \approx 0, \quad (60)$$

$$\phi_{,tt} + \frac{2r_{,t}\phi_{,t}}{r} \approx 0 \Leftrightarrow \phi_{,t} \approx k_1 \cdot r^{-2} + \text{Const}, \quad (61)$$

$$\psi_{,tt} + \frac{2r_{,t}\psi_{,t}}{r} \approx 0 \Leftrightarrow \psi_{,t} \approx k_2 \cdot r^{-2} + \text{Const}. \quad (62)$$

As the singularity is approached, $r_t < 0$ and ϕ_t is also negative. (Refer to the above arguments in the beginning of this section.) Thus, Eq. (61) implies that $\phi_{tt} < 0$. Therefore, ϕ will be accelerated to $-\infty$. Correspondingly, f' approaches zero. Similar arguments can be applied to other equations above. Then, the dynamical system approaches an attractor ($r \rightarrow 0, \sigma = -\infty, f' \rightarrow 0, \psi = -\infty$).

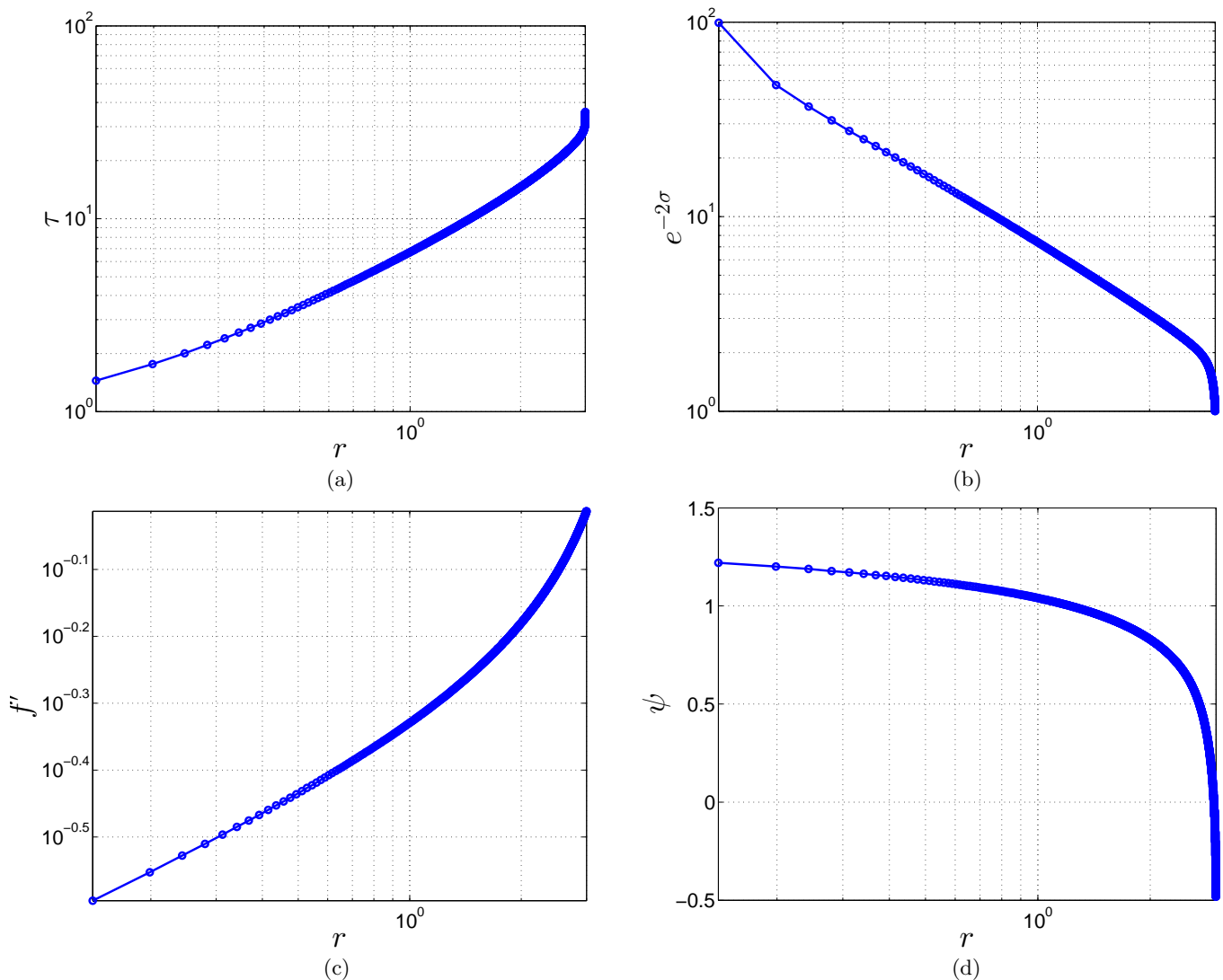


FIG. 6: Kasner solution of the metric components and the scalar fields as one approaches the singularity. The range for the spatial coordinate is $x \in [0, 22]$, and the solution shown in this figure is for $(x = 3, t = t)$, where t is the coordinate time. The quantity τ is defined as follows: τ is set to be equal to zero as one hits the singularity and $d\tau = -e^{-2\sigma} dt$. Near the singularity, we have: (a) $r \propto \tau^{\beta_1}$, (b) $e^{-2\sigma} \propto r^{\beta_2} + \text{Const.}$, (c) $\phi \propto q_1 \ln r + \text{Const.} \Leftrightarrow f' \propto r^{\sqrt{2/3}\kappa q_1}$, (d) $\psi \propto q_2 \ln r + \text{Const.}$ β_1 , β_2 , q_1 , and q_2 are constant parameters.

V. TEST SCALAR FIELDS

The statement that spherical collapse in general relativity can end up with a Schwarzschild black hole has been verified by various numerical simulations. Hawking showed that stationary black holes as the final states of Brans-Dicke collapses are also the solutions of general relativity [13]. This conclusion has been numerically confirmed in Refs. [17, 18, 19]. One may wonder what will happen in collapse in scalar-tensor theories (including $f(R)$ theory), when the global minimum of the potential has a positive value. The static black hole in this circumstance has a de Sitter-Schwarzschild solution. Therefore, the spherical collapse in $f(R)$ theory may also end up with a de Sitter-Schwarzschild black hole. It is

not convenient to check this issue via a long-time simulation in the double-null coordinate. Alternatively, one can study this problem in the following approximate but simpler way. Noting that the mass of the black hole does not change much after the main stage of the collapse, and that the contribution from the dark energy can be neglected, we approximately take the black hole as a stationary Schwarzschild black hole, and study the dynamics of two test scalar fields $\chi \equiv f'$ and ψ in a Schwarzschild background.

The dynamics of a free cosmological scalar field near the horizon of a small black hole is explored analytically in Ref. [42]. Generalized circumstances of a lightly and a heavily massive scalar fields were analyzed in Ref. [43]. In this paper, we use the same method described in Ref. [43]

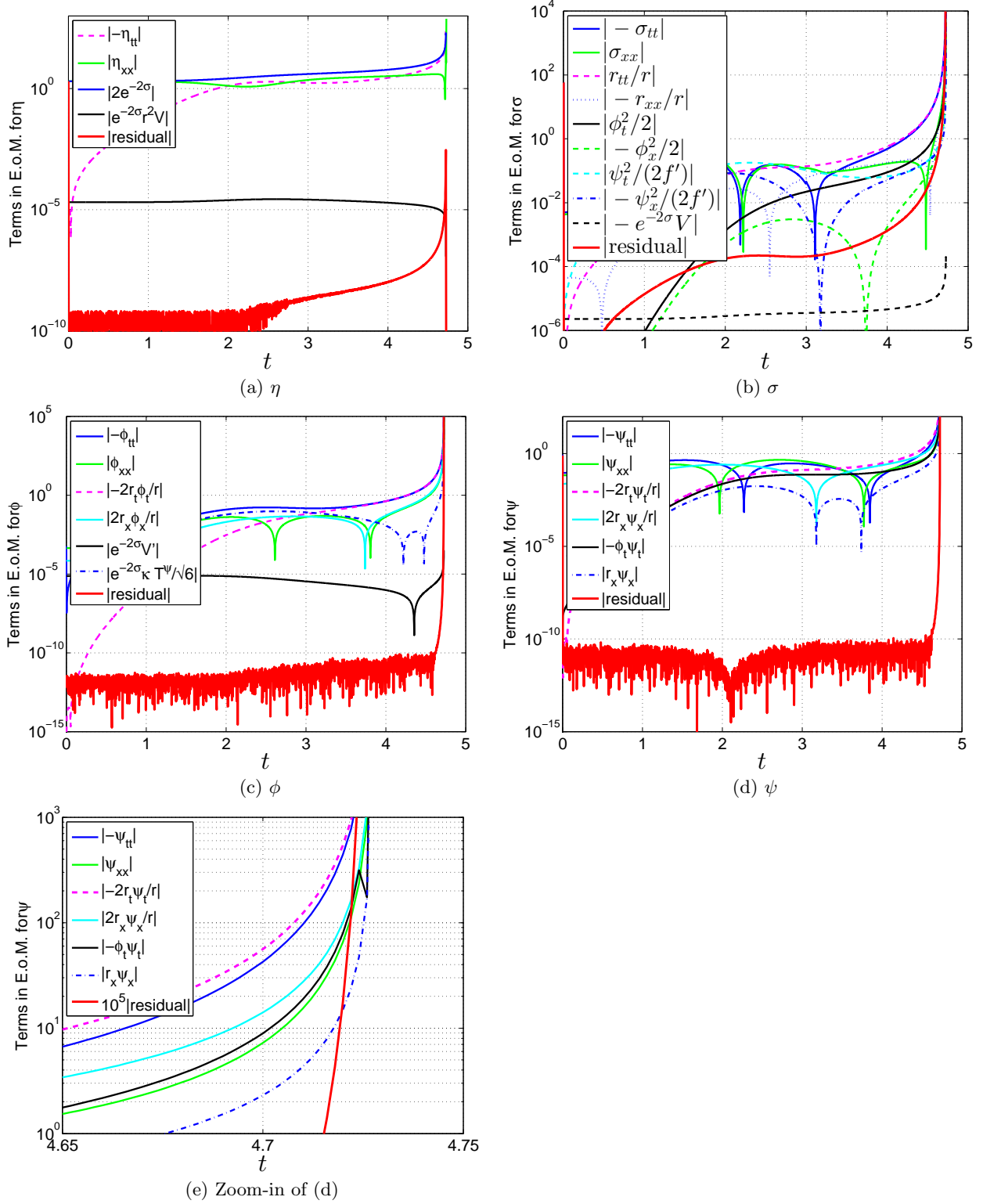


FIG. 7: (Color online) The numerical solutions of the metric components and the scalar fields near the singularity. The range for the spatial coordinate is $x \in [0, 22]$, and the solution shown in this figure is for $(x = 3, t = t)$, where t is the coordinate time. Near the singularity, in the equations of motion, the spatial derivative terms are negligible, the equations of motion are decoupled and transits from partial differential equations into ordinary differential equations with respect to the coordinate time t , and the contributions from the matter fields are also negligible. (a): The equation of motion for η (28) becomes $-\eta_{tt} \approx 2e^{-2\sigma}$. (b): The equation of motion for σ (29) becomes $\sigma_{tt} - r_{tt}/r \approx 0$. (c): The equation of motion for ϕ (30) becomes $\phi_{tt} + 2r_t\phi_t/r \approx 0$. (d) and (e): The equation of motion for ψ (31) becomes $\psi_{tt} + 2r_t\psi_t/r \approx 0$.

to explore the dynamics of two scalar fields χ and ψ after the main stage of the collapse. We study this problem

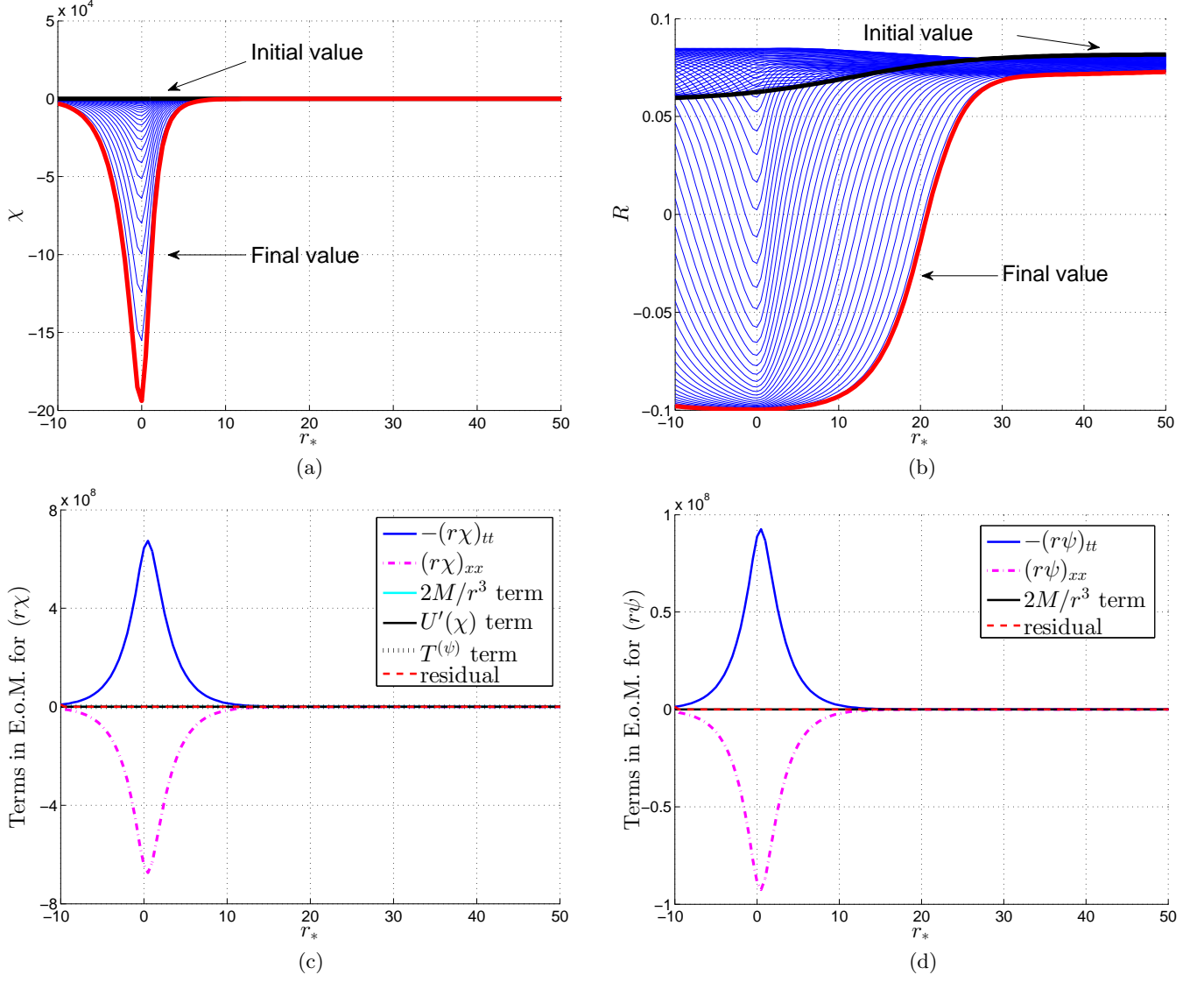


FIG. 8: (Color online) Evolution of scalar fields in Schwarzschild background in Jordan frame. χ can cross zero and goes to $-\infty$. Correspondingly, the Ricci scalar R approaches to $-\Lambda$, which is a pole for $U(\chi)$ [See Eqs. (5) and (22)-(24)]. In (c), $(r\chi)_{xx}$ refers to $\partial^2(r\chi)/\partial r_*^2$.

in a Schwarzschild metric with the tortoise coordinate, $r_* = r + 2M \ln(r/M - 2)$, where r is the usual area radius and M is the mass of the black hole. In the simulations of the spherical collapse, we transformed $f(R)$ gravity from Jordan frame into Einstein frame, so as to avoid the instability from the second-order derivatives of f' . However, we can use Jordan frame directly in the exploration of the dynamics of scalar fields in a fixed metric background. In Jordan frame, the equation of motion for χ is described by Eq. (3). The dynamics of the massless scalar field ψ is defined by

$$\square\psi = 0.$$

In the Schwarzschild metric with the tortoise coordinate,

the equations of motion for χ and ψ become, respectively,

$$\left[\frac{\partial^2}{\partial r_*^2} - \frac{\partial^2}{\partial t^2} - \left(1 - \frac{2M}{r} \right) \frac{2M}{r^3} \right] (r\chi(t, r)) - \left(1 - \frac{2M}{r} \right) \left[U'(\chi) + \frac{8\pi G}{3} T^{(\psi)} \right] = 0, \quad (63)$$

$$\left[\frac{\partial^2}{\partial r_*^2} - \frac{\partial^2}{\partial t^2} - \left(1 - \frac{2M}{r} \right) \frac{2M}{r^3} \right] (r\psi(t, r)) = 0. \quad (64)$$

If the mass of χ is heavy enough, one would expect that the scalar field χ would oscillate near the minimum of the potential, and eventually stop at the minimum. The field ψ would spread out. We replace the potential by $U(\chi) = m^2(\chi - \chi_0)$, and run the numerical simulations.

The results show that when m is large enough, the field χ does stop at the minimum χ_0 in the end as expected, and the field ψ disperses. In the collapse in $f(R)$ gravity, after the main stage of the collapse, the field χ becomes very light, and a small perturbation can push χ to either limit of the potential: at the right limit, $\chi \rightarrow 1$ [44], and at the left limit, $\chi \rightarrow -\infty$. We performed the simulations of χ and ψ in Jordan frame where $U'(\chi)$ is described by Eq. (5). The results, plotted in Fig. 8, show that χ can cross $\chi = 0$ without difficulty. The Ricci scalar R approaches the limit $-\Lambda$ as χ goes to $-\infty$. In this test, Λ is set to -0.1 . Regarding the final state of the collapse in $f(R)$ theory, it is possible that after some oscillations, χ stays at the minimum and ψ spreads out. The further exploration of this problem is underway.

VI. CONCLUSIONS

Spherical scalar collapse in $f(R)$ gravity was simulated in this paper. The results showed that a black hole formation was obtained. The dynamics of the metric components, the scalar degree of freedom f' , and a physical scalar field during the collapse process, including near the singularity, was studied. The results confirmed the BKL conjecture.

The dark-energy-oriented $f(R)$ theory is a modification of general relativity at low-curvature scale. Inside a star whose matter density is much greater than the dark energy density and whose radius is large enough, $f(R)$ gravity is reduced to general relativity and the modification term is negligible. However, near and inside the horizon of a black hole, the scalar curvature is very low, compared to the matter density of the star before the collapse. Then, although gravity is very strong near and inside the horizon of a black hole, the modification term takes effect and even becomes dominant in the function $f(R)$, and the field f' becomes very light. Consequently, the force from the potential is negligible compared to the gravity. Then, f' crosses its de Sitter value, and approaches zero. Therefore, the solution of the dynamical collapse is quite different from the de Sitter-Schwarzschild solution. We will simulate the collapse directly in Jordan frame later, and check whether

f' can cross $f' = 0$ or not.

Near the singularity, in the equations of motion for the metric components, only the terms containing the time derivatives of the metric components remain, and all other terms are negligible. In the equation of motion for scalar field ϕ (or ψ), only the terms containing the time derivatives of ϕ (or ψ) and of the metric components are important. The metric components and the scalar fields f' and ψ are described by Kasner solution. These results supported the BKL conjecture well.

The collapse in Brans-Dicke theory can make a Schwarzschild black hole, with the leftover of the Brans-Dicke field being scattered to infinity. One may expect that the scalar collapse in $f(R)$ theory can end up with a de Sitter-Schwarzschild black hole. We simulated the evolution of two test scalar fields in a fixed Schwarzschild background in Jordan frame. The results show that f' does cross $f' = 0$ without difficulty, and is stopped before the pole ($f' = -\infty, R = -\Lambda$). Due to the lightness of f' , it remains not trivial to study the final state of the collapse in $f(R)$ theory in this approach. This problem will be explored further.

In the studies of the cosmological dynamics and local tests of $f(R)$ theory, a lot of attention has been drawn to the right side and the minimum area of the potential. In the early Universe, the scalar field f' is coupled to the matter density, and is close to 1. In the later evolution, f' goes down towards the minimum of the potential, oscillates, and eventually stops at the minimum. In the oscillation epoch, f' does not deviate too far from the minimum. However, in the collapse process towards a black hole formation, the strong gravity from the black hole pulls f' to a distant place in the left direction from the minimum. Consequently, the left side of the potential needs more care in the collapse problem.

Acknowledgments

This work was supported by the Discovery Grants program of the Natural Sciences and Engineering Research Council of Canada. The authors would like to thank Matthew W Chopuik, Tony Chu, and Levon Pogolian for useful discussions.

-
- [1] A. A. Starobinsky, “A new type of isotropic cosmological models without singularity,” *Phys. Lett. B* **91**, 99 (1980).
 - [2] M. Milgrom, “A modification of the Newtonian dynamics as a possible alternative to the hidden mass hypothesis,” *Astrophys. J.* **270**, 365 (1983).
 - [3] S. M. Carroll, V. Duvvuri, M. Trodden, and M. S. Turner, “Is Cosmic Speed-Up Due to New Gravitational Physics?” *Phys. Rev. D* **70**, 043528 (2004). [[arXiv:astro-ph/0306438](#)]
 - [4] W. Hu and I. Sawicki, “Models of $f(R)$ Cosmic Acceleration that Evade Solar-System Tests,” *Phys. Rev. D* **76**, 064004 (2007). [[arXiv:0705.1158v1 \[astro-ph\]](#)]
 - [5] A. A. Starobinsky, “Disappearing cosmological constant in $f(R)$ gravity,” *JETP Letter*, **86**, 157 (2007). [[arXiv:0706.2041v2 \[astro-ph\]](#)]
 - [6] T. P. Sotiriou and V. Faraoni, “ $f(R)$ Theories Of Gravity,” *Rev. Mod. Phys.* **82**, 451 (2010). [[arXiv:0805.1726v4 \[gr-qc\]](#)]
 - [7] A. D. Felice and S. Tsujikawa, “ $f(R)$ Theories,” *Living Rev. Relativity* **13**, 3 (2010). [[arXiv:1002.4928v2 \[gr-qc\]](#)]
 - [8] B. K. Berger, “Numerical Approaches to Spacetime

- Singularities*,” Living Rev. Relativity **5**, 1 (2002). [arXiv:gr-qc/0201056]
- [9] P. S. Joshi, “Gravitational Collapse and Spacetime Singularities,” (Cambridge University Press, Cambridge, UK, 2007).
- [10] P. S. Joshi, “Recent developments in gravitational collapse and spacetime singularities,” Int. J. Mod. Phys. D, **20**, 2641 (2011). [arXiv:1201.3660 [gr-qc]]
- [11] M. Henneaux, D. Persson, and P. Spindel, “Spacelike Singularities and Hidden Symmetries of Gravity,” Living Rev. Relativity **11**, 1 (2008). [arXiv:0710.1818 [hep-th]]
- [12] R. Ruffini and J. A. Wheeler, “Introducing the black hole,” Phys. Today **24**(1), 30 (1971).
- [13] S. W. Hawking, “Black holes in the Brans-Dicke theory of gravitation,” Comm. Math. Phys. **25**, 167 (1972).
- [14] J. D. Bekenstein, “Novel ‘no-scalar-hair’ theorem for black holes,” Phys. Rev. D **51**, R6608 (1995).
- [15] T. P. Sotiriou and V. Faraoni, “Black holes in scalar-tensor gravity,” Phys. Rev. Lett. **108**, 081103 (2012). arXiv:1109.6324v2 [gr-qc]
- [16] J. R. Oppenheimer and H. Snyder, “On Continued Gravitational Contraction,” Phys. Rev. **56**, 455 (1939).
- [17] M. Shibata, K. Nakao, and T. Nakamura, “Scalar-type gravitational wave emission from gravitational collapse in Brans-Dicke theory: Detectability by a laser interferometer,” Phys. Rev. D **50**, 7304 (1994).
- [18] M. A. Scheel, S. L. Shapiro, and S. A. Teukolsky, “Collapse to Black Holes in Brans-Dicke Theory: I. Horizon Boundary Conditions for Dynamical Spacetimes,” Phys. Rev. D **51**, 4208 (1995). [arXiv:gr-qc/9411025]
- [19] M. A. Scheel, S. L. Shapiro, and S. A. Teukolsky, “Collapse to Black Holes in Brans-Dicke Theory: II. Comparison with General Relativity,” Phys. Rev. D **51**, 4236 (1995). [arXiv:gr-qc/9411026]
- [20] T. Hertog, “Towards a Novel no-hair Theorem for Black Holes,” Phys. Rev. D **74**, 084008 (2006). [arXiv:gr-qc/0608075]
- [21] E. Berti, V. Cardoso, L. Gualtieri, M. Horbatsch, and U. Sperhake, “Numerical simulations of single and binary black holes in scalar-tensor theories: circumventing the no-hair theorem,” Phys. Rev. D **87**, 124020 (2013). [arXiv:1304.2836 [gr-qc]]
- [22] J. A. R. Cembranos, A. de la Cruz-Dombriz, and B. M. Nunez, “Gravitational collapse in $f(R)$ theories,” J. Cosmol. Astropart. Phys. **04** (2012) 021. arXiv:1201.1289 [gr-qc]
- [23] M. Kopp, S. A. Appleby, I. Achitouv, and J. Weller, “Spherical collapse and halo mass function in $f(R)$ theories,” Phys. Rev. D **88**, 084015 (2013). arXiv:1306.3233 [astro-ph.CO]
- [24] A. Barreira, B. Li, C. Baugh, and S. Pascoli, “Spherical collapse in Galileon gravity: fifth force solutions, halo mass function and halo bias,” arXiv:1308.3699 [astro-ph.CO]
- [25] V. A. Belinski, I. M. Khalatnikov, and E. M. Lifshitz, “Oscillatory Approach to a Singular Point in the Relativistic Cosmology,” Adv. Phys. **19**, 525 (1970).
- [26] E. Kasner, “Geometrical theorems on Einsteins cosmological equations,” Amr. J. Math. **43**, 217 (1921).
- [27] J. Wainwright and A. Krasinski, “Republication of: Geometrical theorems on Einsteins cosmological equations (By E. Kasner),” Gen. Relativ. Gravit. **40**, 865 (2008).
- [28] B. K. Berger, D. Garfinkle, J. Isenberg, V. Moncrief, and M. Weaver, “The Singularity in Generic Gravitational Collapse Is Spacelike, Local, and Oscillatory,” Mod. Phys. Lett. A **13**, 1565 (1998). [arXiv:gr-qc/9805063]
- [29] D. Garfinkle, “Numerical Simulations of Generic Singularities,” Phys. Rev. Lett. **93**, 161101 (2004). [arXiv:gr-qc/0312117]
- [30] D. Garfinkle, “Examining Gravitational Collapse With Test Scalar Fields,” Classical Quantum Gravity **27**, 165019 (2010). [arXiv:1004.3569 [gr-qc]]
- [31] A. Ashtekar, A. Henderson, and D. Sloan, “A Hamiltonian Formulation of the BKL Conjecture,” Phys. Rev. D **83**, 084024 (2011). [arXiv:1102.3474 [gr-qc]]
- [32] D. Christodoulou, “Bounded Variation Solutions of the Spherically Symmetric Einstein-Scalar Field Equations,” Commun. Pure Appl. Math. **46**, 1131 (1993).
- [33] J. Khoury and A. Weltman, “Chameleon Fields: Awaiting Surprises for Tests of Gravity in Space,” Phys. Rev. Lett. **93**, 171104 (2004). [arXiv:astro-ph/0309300v3]
- [34] J. Khoury and A. Weltman, “Chameleon Cosmology,” Phys. Rev. D **69**, 044026 (2004). [arXiv:astro-ph/0309411v2]
- [35] J.-Q. Guo and A. V. Frolov, “Cosmological dynamics in $f(R)$ gravity,” arXiv:1305.7290 [astro-ph.CO]
- [36] J.-Q. Guo, “Solar system tests of $f(R)$ gravity,” arXiv:1306.1853 [astro-ph.CO]
- [37] A. V. Frolov, “Is It Really Naked? On Cosmic Censorship in String Theory,” Phys. Rev. D **70**, 104023 (2004). [arXiv:hep-th/0409117]
- [38] F. Pretorius, “Numerical Relativity Using a Generalized Harmonic Decomposition,” Classical Quantum Gravity **22**, 425 (2005). [arXiv:gr-qc/0407110]
- [39] E. Sorkin and T. Piran, “Effects of Pair Creation on Charged Gravitational Collapse,” Phys. Rev. D **63**, 084006 (2007). [arXiv:gr-qc/0009095v2]
- [40] S. Golod and T. Piran, “Choptuik’s Critical Phenomenon in Einstein-Gauss-Bonnet Gravity,” Phys. Rev. D **85**, 104015 (2012). [arXiv:1201.6384v3 [gr-qc]]
- [41] V. A. Belinsky and I. M. Khalatnikov, “Effect of scalar and vector fields on the nature of the cosmological singularity,” Sov. Phys. JETP **36**, 591 (1973). [Zh. Eksp. Teor. Fiz. **63**, 1121 (1972).]
- [42] T. Jacobson, “Primordial black hole evolution in tensor-scalar cosmology,” Phys. Rev. Lett. **83**, 2699 (1999). [arXiv:astro-ph/9905303]
- [43] A. V. Frolov and L. Kofman, “Inflation and de Sitter Thermodynamics,” J. Cosmol. Astropart. Phys. **05** (2003) 009. [arXiv:hep-th/0212327]
- [44] A. V. Frolov, “A Singularity Problem with $f(R)$ Dark Energy,” Phys. Rev. Lett. **101**, 061103 (2008). [arXiv:0803.2500v2 [astro-ph]]